Anisotropic Shock Propagation in Single Crystals

J.H. Eggert, D.G. Hicks, P.M. Celliers, D.K. Bradley, J.E. Cox, W.G. Unites, G.W. Collins,*
Lawrence Livermore National Laboratory, Livermore, CA, USA, eggert1@llnl.gov
R.S. McWilliams, R. Jeanloz, University of California, Berkeley, CA, USA
S. Bruygoo, P. Loubeyre, Commissariat à l'Energie Atomique, Bruyères-le-Châtel, France

Introduction

Most single-crystal shock experiments have been performed in high-symmetry directions while the nature of shock propagation in low-symmetry directions remains relatively unstudied. It is well known that small-amplitude, linear acoustic waves propagating in low-symmetry directions can focus and/or form caustics (Wolfe, 1995). In this report we provide evidence for similar focusing behavior in nonlinear (shock) waves propagating in single crystals of silicon and diamond. Using intense lasers, we have driven non-planar (divergent geometry) shock waves through single-crystals of silicon or diamond and into an isotropic backing plate. On recovery of the backing plates we observe a depression showing evidence of anisotropic plastic strain with well-defined crystallographic registration. We observe 4-, 2-, and 3-fold symmetric impressions for [100], [110], and [111] oriented crystals respectively.

Experimental

Shock waves generated by intense lasers at the JANUS laser (Lawrence Livermore National Laboratory, CA) and at the OMEGA laser (University of Rochester, NY) were driven through single crystal silicon or diamond targets of known orientation attached to an isotropic metal backing plate. Silicon targets (figure 1a) were wafers (1 mm thick, >5 mm across) epoxied onto stainless steel backing plates (6 mm thick); diamond targets (figure 1b) consisted of the thick anvil used in pre-compressed diamond-anvil cell laser shock experiments (1 mm culet, 3 mm table, 1.2 mm thick) placed on tungsten-carbide backing plates (5 mm thick) (Loubeyre, 2004). A ~15 μm CH ablator was evaporated onto the laser ablation surface to increase the efficiency of shock wave generation. The laser was focused to a 300 μm diameter spot using laser energies from 60-2000J and pulse durations of 1-4 ns. Since the propagation time through the samples is ~100 ns, the shocks are unsupported and rapidly decaying. We estimate that the shock pressures within the crystals range from several Mbars to several hundred kbar. After the experiments the single-crystal samples broke apart and were usually lost but the backing plates were

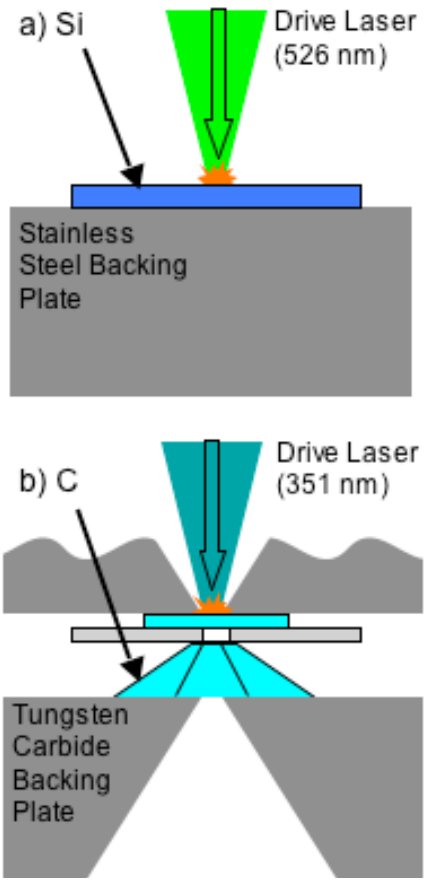

Figure 1, Target configurations.

generally recovered intact.

The recovered backing plates showed anisotropic deformations that were strongly correlated to the crystallographic orientations of the single crystals. We used a WYCO NT-2000 white light interference profilometer to measure the depth of this indentation to a resolution of 100 nm with a spatial resolution of 10 μm. Figure 1 shows three of these WYKO profiles taken on three silicon orientations. There is obvious 4-, 2-, and 3-fold symmetry and clear registration with the silicon orientations as shown in figure. Similar profiles were observed in every shot we performed (15 silicon, 26 diamond) except when the tungsten carbide backing plates occasionally fractured and the information was lost.

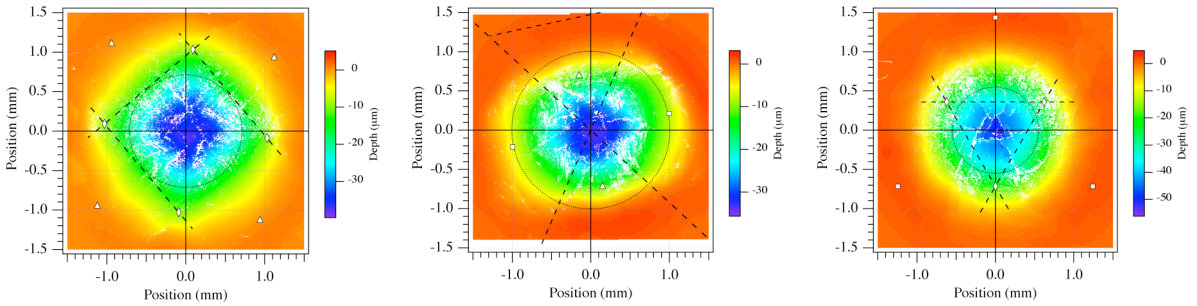

Figure 2, WYKO indention-depth images of single crystal silicon from three crystal orientations, [100], [110], and [111] (4 ns laser drive with energies of 333 J, 276 J, and 327 J). High symmetry directions from shock origin are shown for [100], [110], and [111] directions by squares, triangles, and diamonds respectively. The dashed lines denote the intersection of {111} planes through the shock origin with the backing plate.

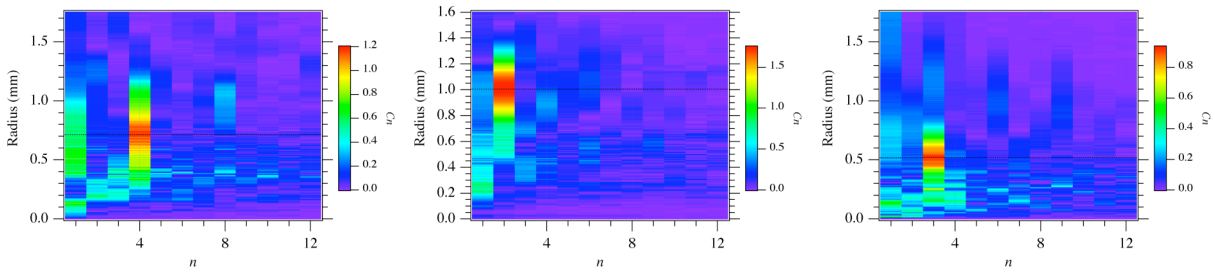

Figure 3, Histograms of the symmetry order parameter C_n for the same three shots shown above. There is relatively little contribution from overtones. The radius of maximum asymmetry is 0.71 mm, 1.01 mm , and 0.52 mm respectively.

In order to quantize the depth profile asymmetry, We define a symmetry order parameter as,

$$C_n = \frac{\int d\theta f(\theta) e^{in\theta}}{2\pi}$$

where $f(\theta)$ is the depth at angle θ. Figure 3 shows bar charts of C_n for the three shots shown in Figure 2. As expected from visual inspection, the shots show distinct 4-, 2-, and 3-fold symmetry with very little overtone contribution.

All of the diamond samples were [100] orientation and were qualitatively similar to the silicon shots as shown in figure 4. While the diamond anvils were generally lost after the shots, we did recover several diamond crystals from very low energy shots. These recovered crystals

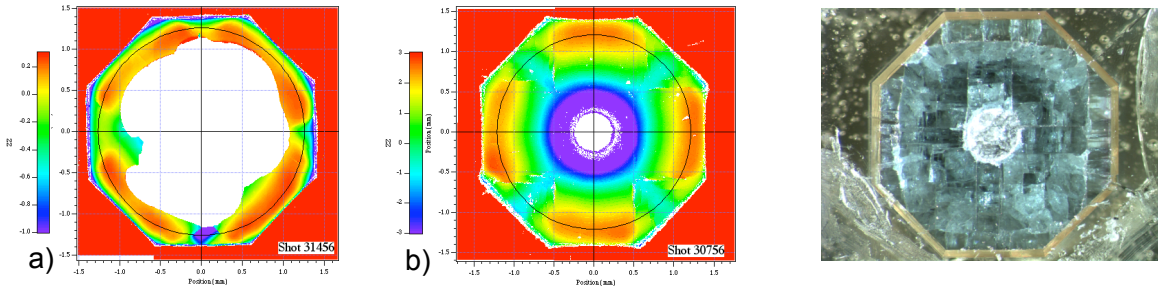

Figure 4. Indentations of [100] diamond into tungsten carbide at different 1 ns laser energies a) E=192.9 J b) E=371.5 J. White regions correspond to the holes in the backing plates. Both a) and b) feature a 4-fold deformation as in the silicon [100] experiments, but b) also contains discontinuous 'steps' due to shearing along fracture planes in diamond. The photograph shows the table of a recovered diamond where fractures along {111} planes are visible.

were highly fractured as shown in figure 4. We unambiguously identified the fractured planes as {111} by carefully measuring the fracture angles. It is not clear whether the observed fracturing of diamond occurred on compression or release of the shock wave and before or after the indentation process. However, we do see evidence of this fracturing as steps in some of the recovered tungsten carbide plates. Figure 4 includes depth images showing the absence (4a) and the presence (4b) of such steps. In two shots we recovered a portion of the diamond anvil allowing us to gain further insight into the nature of the {111} fractures. The fractured anvils were too fragile for us to obtain high quality photos, but a schematic rendition of our observations including the observed correlation with the backing plate indentation is shown in figure 5.

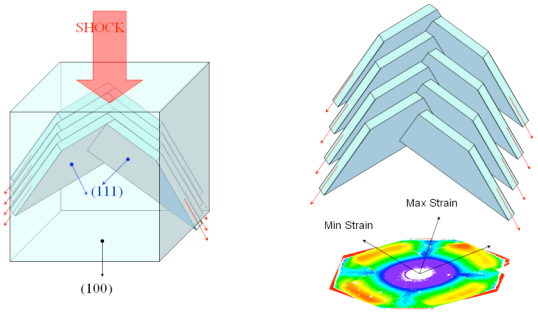

Figure 5, Schematic illustration of two partially recovered highly fractured diamonds.

Discussion

Ultimately, when we measure the indention depth in a backing plate due to shock propagation, we are measuring the plastic deformation of the backing plate integrated over time. This can be expressed in terms of the z-component of the backing plate particle velocity,

$$d = \iint_{HEL} U_{p,x}(t)\,dtdz.$$

The limits of integration are taken over the time (as a function of z) that the pressure in the backing plate is above the elastic limit of the backing plate (compressive strength of stainless steel is about 10-20 kbar, of tungsten carbide is about 40 kbar). Obviously, given our complex loading geometry and time history, it is unreasonable to attempt to evaluate this integral, but it seems reasonable to expect that a deeper indention implies a stronger shock. Thus, we have evidence in our data that single crystal diamond and silicon redistribute shock strength according to the crystallographic direction of propagation. The mechanism for this shock "focusing" is likely due to either elastic or elastic/plastic anisotropy, although other mechanisms may very well exist.

Elastic anisotropy is described by the elastic moduli of a crystal. In general, if the moduli are not perfectly isotropic then the group and phase velocities of linear elastic waves are not parallel. This gives rise to an effect called "phonon focusing" that has been observed in both silicon (Wolfe, 1995) and diamond (Hurley, 1984). The resultant singularities in wave intensity are very similar to the visible light caustics commonly seen at the bottom swimming pools. Phonon focusing has only been observed in the linear regime where wave velocities are independent of amplitude, and in this regime good analytical methods are available to calculate the response in detail (Every, 1980). The more complicated non-linear regime where shocks form has not received similar attention. In fact, the far simpler case of caustic formation due to convergent rays in the non-linear regime has been studied for nearly 50 years with no simple treatment yet available (Whitham, 1956; Monica, 2001). It is possible that we are seeing the effects of non-linear wave focusing associated with differences in the group and phase velocities.

Alternatively, it is possible that the elastic/plastic anisotropy of the materials is responsible for our observations. In fcc crystals there are 12 {111} <110> slip systems. For a given stress one or more of these systems will have the maximum resolved shear stress. Thus, the stress required to initiate dislocation motion will depend on the stress orientation. This gives rise to the orientation dependence of the Hugoniot elastic limit observed in silicon (Gust, 1971)) referred to here as elastic/plastic anisotropy. Elastic/plastic anisotropy has been studied theoretically for shocks in beryllium (Johnson, 1972) where it has been noted that significant transverse material motion and multiple plastic-wave propagation can occur in non-symmetric propagation directions. Multiple plastic-wave propagation was subsequently observed and interpreted as due to elastic/plastic anisotropy in beryllium (Pope, 1974). Unfortunately, it is unclear how the shock strength would be affected by elastic/plastic anisotropy in a non-planar shock.

Conclusions

We have propagated non-planar (divergent geometry), laser-driven shock waves through single-crystals of silicon and diamond and into an isotropic backing plate. On recovery of the backing plates we observe a depression showing evidence of anisotropic plastic strain with well-defined crystallographic registration. We observe 4-, 2-, and 3-fold symmetric impressions for [100], [110], and [111] oriented crystals respectively. We propose that this anisotropy is evidence of shock-strength anisotropy in these single crystals. Two potential explanations are suggested, elastic and elastic/plastic anisotropy, but we cannot yet conclusively identify the mechanism.

References

EVERY A.G., 1980, General closed-form expressions for acoustic waves in elastically anisotropic solids. *Phys. Rev. B*, **22**, 1746-1760.

GUST W.H., and Royce E.B., 1971, Axial yield strengths and two successive phase transition stresses for crystalline silicon. *J. Appl. Phys.*, **42**, 1897-1905.

HURLEY D.C., Every A.G., and Wolfe J.P., 1984. Ballistic phonon imaging of diamond. *J. Phys. C*, **17**, 3157-3166.

JOHNSON J.N., 1972, Calculation of plane-wave propagation in anisotropic elastic-plastic solids. *J. Appl. Phys*. **43**, 2074-2082.

LOUBEYRE P., Celliers P.M., Hicks D.G., Henry E., Dewaele A., Pasley J., Eggert J., Koenig M., Occelli F., Lee K.M., Jeanloz R., Neely D., Benuzzi-Mounaix A., Bradley D., Bastea M., Moon S., and Collins G.W., 2004, Coupling static and dynamic compressions: First measurements in dense hydrogen. *High Pres. Res.* **24**, 25-31.

MONICA A., and Prasad P., 2001, Propagation of a curved weak shock. *J. Fluid Mech*. **434**, 119-151.

POPE L.E., and Johnson J.N., 1974, Shock-wave compression of single-crystal beryllium. *J. Appl. Phys*. **46**, 720-727.

WHITHAM G.B., 1956, On the propagation of weak shock waves. *J. Fluid Mech.* **1**, 290-318.

WOLFE J.P., and Hauser M.R., 1995, Acoustic wavefront imaging. *Annalen der Physik*, **4**, 99-126.